Journal of Environmental Management 327 (2023) 116804

Contents lists available at ScienceDirect

Journal of Environmental Management

journal homepage: www.elsevier.com/locate/jenvman

Research article

Predicting future coastal land use/cover change and associated sea-level impact on habitat quality in the Northwestern Coastline of Guinea-Bissau

Namir Domingos Raimundo Lopes [a,b], Tianxin Li [a,b,*], Peng Zhang [c], Nametso Matomela [a,b], Harrison Odion Ikhumhen [d], Rui M. Sá [e]

[a] School of Energy and Environmental Engineering College, University of Science and Technology Beijing, Beijing, 100083, China
[b] Beijing Key Laboratory of Resource-oriented Treatment of Industrial Pollutants, Beijing, 100083, PR China
[c] State Environmental Protection Key Laboratory of Quality Control in Environmental Monitoring, China National Environmental Monitoring Centre, Beijing, 100012, China
[d] Key Laboratory of Ministry of Education for Coastal Wetland Ecosystems, College of the Environment and Ecology, Xiamen University, Fujian, 361102, China
[e] Centre for Public Administration & Public Policies (CAPP) ISCSP, University of Lisbon, Lisboa, 1300-663, Portugal

ARTICLE INFO

Keywords:
Remote sensing
Change analysis
Driving forces
Future prediction
Coastal protection

ABSTRACT

The assessment of coastal land use/cover (LULC) change is one of the most precise techniques for detecting spatio-temporal change in the coastal system. This study, integrated Land Change Modeler, Habitat Quality Model, and Digital Shoreline Analysis System, to quantify spacio-temporal coastal LULC change and driving forces between 2000 and 2020. Combined the CA-Markov Model with Sea Level Affecting Marshes Model (SLAMM), merged local SLR data with future representative concentration pathway (RCP8.5) scenarios, and predicted future coastal LULC change and associated sea-level rise (SLR) impact on the coastal land use and habitat quality in short-, medium- and long-term. The study area had significant coastal LULC change between 2000 and 2020. The tidal flats, whose change was driven mainly by sea level, registered a total net gain of 57.93 km^2. We also observed the significant loss of developed land whose change was influenced by tidal flat with a total loss of −75.58 km^2. The tidal flat will experience a stunning net gain of 80.55 km^2 between 2020 and 2060, making developed land the most negatively impacted land in the study area. The study led to the conclusion that the uncontrolled conversion of saltmarshes, mixed-forest, and mangroves into agriculture and infrastructures were the main factors affecting the coastal systems, including the faster coastal erosion and accretion observed during a 20-year period. The study also concluded that a low coastal elevation of −1 m and a slope of less than 2° have contributed to coastal change. Unprecedented changes will unavoidably pose a danger to coastal ecological services, socioeconomic growth, and food security. Timely efforts should be made by establishing sustainable mitigation methods to avoid the future impact.

1. Introduction

The coastal LULC change disrupts hydrological and sedimentary regimes, largely limiting the form and biomass of coastal ecosystems (Han et al., 2015). It is recognized that significant changes in coastal LULC can have a significant impact on regional climate, water balance, socioeconomic activity, ecosystem stability, and biodiversity (Abdullah et al., 2022; Alam et al., 2019; Kindu et al., 2013). Anthropogenic activity is one of the main driver of the dramatically rising change of coastal LULC (Yohannes et al., 2021). Gains in agriculture and losses in forestry during the past 300 years have been determined to categorize the worldwide LULC change route (Latham et al., 2002; Meyer and Turner, 1992). It has been recognized that a major factor influencing LULC changes in Africa is the growth of agricultural area impacted by a rapidly expanding population. Up to the early 1900s, industrialization and agricultural development caused significant deforestation in the majority of developed countries, including the United States and Europe (Hailu et al., 2020). Additionally, LULC change has grown to be a major concern in many coastal ecosystems across the world (Belward and Skøien, 2015; Niedertscheider et al., 2014). Climate change intensifies

* Corresponding author. School of Energy and Environmental Engineering College, University of Science and Technology Beijing, Beijing, 100083, China.
E-mail addresses: lopesnamir@hotmail.com (N.D.R. Lopes), tianxinli@ustb.edu.cn (T. Li), zhangpeng@cnemc.cn (P. Zhang), hikhumhen@xmu.edu.cn (H.O. Ikhumhen), ruimoutinhosa@gmail.com (R.M. Sá).

https://doi.org/10.1016/j.jenvman.2022.116804
Received 25 August 2022; Received in revised form 7 November 2022; Accepted 14 November 2022
Available online 1 December 2022
0301-4797/© 2022 Elsevier Ltd. All rights reserved.

ocean circulation and coastal risks, which has decreased global land area, potential production, and ecosystem health (Sajjad et al., 2020; Wu and Han, 2019). The danger of climate change, particularly sea level rise and its effects on low-lying coastlines, has drawn attention on a global scale over the past few decades (IPCC, 2007). In the coming decades, sea level rise and storm surge effects are anticipated to increase coastal erosion and accretion, which pose a serious threat to the quality of coastal ecosystems in the short, medium, and long terms (Djouder and Boutiba, 2017; Ghoussein et al., 2018). According to a recent study by Lopes et al. (2022) in the Northwestern Coastline of Guinea-Bissau, the sea level has risen at a rate of 8.79 mm/year over the last 15 years. From 1995, it is predicted that Guinea-Bissau's SLR will be 0.13 m, 0.35 m, 0.72 m, and 1.22 m in 2025, 2050, 2075, and 2100, respectively. The impacts are projected to cause considerable changes in coastal LULC, which will have an impact on the quality of coastal ecosystems and community livelihood (Sajjad et al., 2020). Understanding the current and future changes in LULC is crucial and necessitates an early assessment due to the increasing coastal pressures (del-Toro and Más-López, 2019).

Predicting coastal LULC change has emerged as a significant factor in several disciplines, such as rural and urban plan modeling and identifying biodiversity hotspots to advance conservation planning efforts (Wang et al., 2020). Environmentalists, conservationists, and urban planners are very concerned with the detection and prediction of coastal LULC change using a GIS-related remote sensing approach because of how it affects the natural ecosystems (Gashaw et al., 2017; Hyandye and Martz, 2017). By providing scientific and trustworthy information for economic development strategy to fulfill social and environmental goals, the forecast can help with land use and conservation planning (Bhuiyan et al., 2012). For instance, Addo (2010) claimed that using remote sensing to map LULC changes could provide important policy recommendations for developing nations' sustainable coastal landscape management. Masrur et al. (2022) concluded that, Multitemporal satellite nighttime light (NTL) as a proxy for human presence in the river network is essential for regularly flood-affected low-lying regions and populous nations, like Bangladesh. Yirsaw et al. (2017) revealed that it is important to employ remote sensing data to track how sea level rise may affect future ecosystem services in Su-Xi-Chang, China. This will help to manage and conserve the area's ecological resources. The most commonly used models in estimating the LULC and habitat quality changes include analytical equation-based models (Shamsi, 2010), Markov models (Yang et al., 2012), hybrid models (Subedi et al., 2013), statistical models (Hyandye et al., 2015) and, cellular models (Singh et al., 2015), InVEST Models. The cellular and Markov chain hybrid model known as the CA-Markov and InVEST Models is the most often utilized among the methodologies discussed above (Xu et al., 2022; Zhao and Peng, 2012). The Sea Level Affecting Marshes Model (SLAMM), which is based on geographic information systems, simulates and predict the key factors impacting shoreline change and coastal LULC (wetlands) at local to regional scales (Craft et al., 2009; Mcleod et al., 2010).

Predicting coastal LULC changes is critical to understanding how the earth interacts, coastal vegetation fragmentation, biodiversity loss, and future management strategies (Al-Tahir and Asim Ali, 2004; Halmy et al., 2015). Although there are still a very small number of studies being conducted globally (Abijith and Saravanan, 2021; Baig et al., 2022; Mazor, 2021), none have yet focused on the Northwestern Coastline of Guinea-Bissau. This region is a designated Ramsar site due to its abundance of biodiversity and one of West Africa's largest and densest mangrove areas (del-Toro and López, 2019; Lopes et al., 2022; Ramsar, 2015). Therefore, this study applied remote sensing related GIS, combining Land Change Modeler (LCM), Habitat Quality Model (HQM), and Digital Shoreline Analysis System (DSAS) to quantify temporal coastal LULC change and investigate the driving forces between 2000 and 2020; combine CA-Markov Model with Sea Level Affecting Marshes Model (SLAMM) and merge the local study area's SLR data with future representative concentration pathway (RCP8.5) scenario to predict future coastal LULC change and associated sea-level rise (SLR) impact on the coastal land use and habitat quality in short-, medium- and long-term in the Northwestern Coastline of Guinea-Bissau (NC-GB). The findings are anticipated to aid policymakers and coastal managers in developing sustainable mitigation and adaptation measures and reinforcing ecological protection to reduce the effects of SLR in the future.

2. Materials and methods

2.1. Study area

Geographically, the study area is situated along Guinea-Bissau's Northwestern Coastline, within the latitude and longitude of 12° 16′ 14″ North and 16° 9′ 57″ West, respectively (Fig. 1). Lowlands that are submerged during high tide (del-Toro et al., 2019; Lopes et al., 2022). It has a tropical climate with temperature variations of 20 °C and 34 °C (Pelissier and Rene, 2004). The NC-GB is home to a variety of natural resources that are important, such as an estuary, rivers, the Varela heavy sand mining area, long sandy beaches, and one of West Africa's largest and most densely populated mangrove reservoirs. These resources provide ideal nesting and breeding habitats for a considerable fish population and other seafood, migratory seabirds, and threatened species like the West African manatee. In addition to its rich natural biodiversity, the area offers tremendous cross-cultural value to the numerous ethnic groups living within its borders, who have engaged in artisanal fishing and agriculture for decades (Ramsar, 2015). Due to its significant natural importance and unique socioeconomic circumstances, this area needed sustained conservation actions (Lopes et al., 2022).

2.2. Data collection and pre-processing

This study used two distinct satellite images (2000–2020). EarthExplorer was used to download the free Landsat images (USGS, 2020). With the use of Pan-sharpened Raster Dataset under Raster processing, ArcToolbox of ArcGIS 10.5, the resolution of Landsat-7 for the year 2000 and Landsat-8 for the year 2020, both at 30 m resolution, was increased to 15 m. These images were utilized as inputs to the CA-Markov and SLAMM models to categorize coastal LULC. The expression times of the images were determined by taking into account seasonal changes from January to April, in accordance with the study area's dry season. Three images of the study area were clipped, mosaicked, and corrected as part of the pre-processing of the images for maximum likelihood supervised classification. The main steps in this study are as follows: (1) Classification and accuracy assessment; (2) Temporal coastal LULC change quantification; (3) Driving forces investigation; (4) Predicting coastal LULC change; and (5) Projecting future impact of SLR on coastal land use and habitat quality. The paradigm of the future prediction procedure is illustrated in Suppl. F1.

2.3. Coastal LULC classification and accuracy assessment

To extract important thematic information, image classification divides all Landsat image pixels into LULC classes (Al-sharif and Pradhan, 2014). After pre-processing the image, the "Maximum Likelihood Classification" algorithm was used for supervised classification (MLC)." For supervised classification, the MLC technique offers a popular optimization algorithm (Richards, 1999). This method offers a strong conceptual foundation and the flexibility to accommodate different types of remote sensing data. The statistical classification-based supervised classification strategy is chosen because it preserves the fundamental characteristics of LULC (Cheruto et al., 2016; Gashaw et al., 2014). According to the "Official Bulletin" Land Act No. 5/98, the LULC classification status used in this study was obtained from the Ministry of Natural Resources of Guinea-Bissau. Text was created on April 23, 1998, and was used as the principal categorization scheme for the 2000 and 2020 images. This

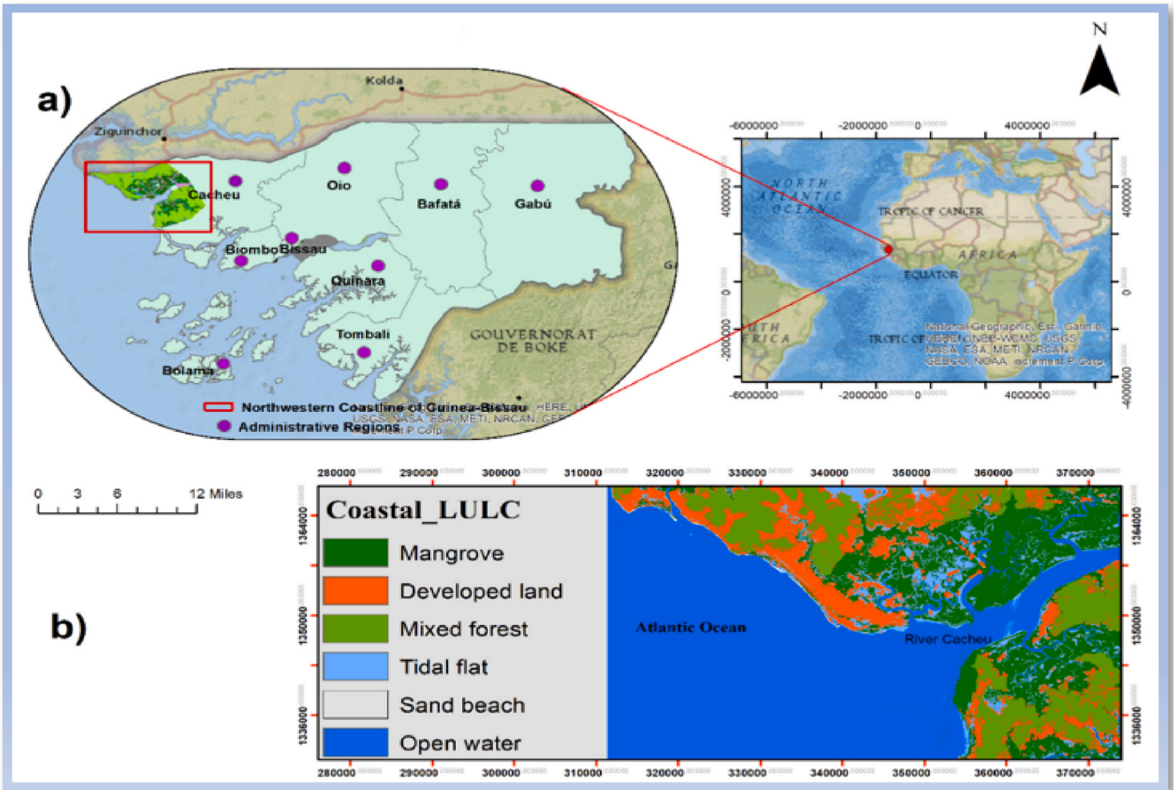

Fig. 1. The location of study area in Africa and Guinea-Bissau based on the open street map and shapefile. a) The located study area in Guinea-Bissau; b) the classified study area map based on six LULC classes using Landsat-8, 15-m resolution.

classification takes six basic classes into account (Table 1). ArcGIS v.10.5 and Idrissi Terrset v.18.31 software was both used to classify images for mapping.

Classification accuracy is a pre-condition for credible change detection (Wang et al., 2020). To evaluate the quality and precision of the images and contrast them with actual field locations, an error matrix and kappa are applied to the final categorized image (Congalton and Green, 2019). This study adopted the Cohen (1968) formula to calculate Kappa coefficient.

2.4. Coastal LULC change quantification

Initial plans for the Land Change Modeler (LCM) in TerrSet IDRISI software included handling ecological and biodiversity assessment as well as LULC alterations (Ghosh et al., 2017; Mazor et al., 2021; Pirasteh et al., 2021). Based on thematic rasters with the same class number and sequential order, the model analyzes LULC changes (Singh et al., 2015). In this section, we quantify coastal LULC changes in NC-GB between 2000 and 2020.

A quick quantitative change assessment is provided by the change analysis through a graphical representation of gains and losses among various LULC classes, as well as the net change and contribution to the net change that each class experienced. Such changes are important for determining the most common transition between classes. The results are displayed in a graphical map using the spatial trend of change (Matlhodi et al., 2021). In this approach, each node served as the foundation for the processing component using a nonlinear activation function. Using the equation created by Hyandye et al. (2015), the neural model output can be achieved given the input data.

Table 1
Land cover classes scheme.

N.	Primary land cover classes	Secondary land cover classes
1	Mangrove	Rhizophora racemosa, Rhizophora mangle, Rhizophora harrisonii, Avicennia germinans, Laguncularia racemosa and Conocarpus erectus.
2	Developed land	Paddy field, horticulture, build up, dry land.
3	Mixed forest	Weeds, Wood Forest, Shrub, Casheu Plantations, broadleaf forests, conifer forests, and riparian.
4	Tidal flat	Mud flat, saltmarsh
5	Sand Beach	Ocean beach
6	Open water	Sea, rivers, streams, ponds, lakes, reservoirs

2.5. Driving forces of coastal LULC change

2.5.1. Socioeconomic drivers

The Habitat Quality Model (HQM) combines information about coastal LULCs and habitat threats (Naturalcapitalproject, 2020). This approach produces two main pieces of information, including the relative amount of various habitat types in a location and changes over time, that help estimate conservation needs (Xiaowei et al., 2015). This assessment was based on socioeconomic factors that directly affected the coastal environment. It was assumed that the more frequent the economic activities are in coastal zones, the worse the land cover and habitat quality in a region become (Yang et al., 2018). For instance, mangroves may be extremely susceptible to risks driven on by agricultural activities but just slightly sensitive to those driven on by tourism. Agriculture and infrastructure, which were included in the HQM as threat variables, were the two key activities that the socioeconomic driver's assessment in this study concentrated on. This study adopted the equation developed by Naturalcapitalproject (2020), to calculate the coastal habitat quality and its sensitivity to the agricultural and infrastructural actions.

2.5.2. Coastal hazards drivers

The DSAS v-5.0 software, add-in for Esri ArcGIS desktop 10.4–10.7, allows users to calculate the rate of change using various historical shoreline positions (Zagórski et al., 2020). This assessment was based on coastal accretion and erosion caused by the accelerated sea level rise between 2000 and 2020. These phenomena have an immediate impact on the condition of the coastal ecosystem. It has been assumed that a region's habitat quality declines when coastal threats increase in frequency. The shorelines, baselines, and transects for selected years were created to calculate the net change (Marfai et al., 2008). By fitting the least-squares regression line to all coastline sites on a transect, the net shoreline measurement (NSM) statistical parameter was chosen to estimate the net change between 2000 and 2020 (Zagórski et al., 2020). This method includes all data, regardless of changes in trend or accuracy. It is calculated using Nicu, 2021 equation.

2.5.3. DEM and slope implication

Topographic, elevation, slope, road distance, stream distance, distance from an urban area, and raster evidence likelihood have all been employed as driving variables in numerous LULC change simulations (Hyandye et al., 2015). In this study, DEM and slope are taken into consideration as potential contributor variables for LULC change, due to the study area's coastal characteristics. These variables measure the numerical transition from one land cover to another. The relevance of these two contributor factors was examined using Cramer's V and P values, which reflect the high correlation between the two variables in the LCM. Cramer's V value, which ranges from 0.0 to 1.0, is a basic statistical indicator correlated between variables. Variables with a Cramer's total V-value of 0.15 or higher are frequently regarded as reasonable contributors, while those with a score of 0.40 or higher are regarded as sufficient contributors for change (Hyandye et al., 2015). Cramer's V cannot accurately represent the prerequisites of science and the complex relationship content; thus, it cannot ensure that the variables function properly. Instead, it merely assists in determining the specific variable included as a contributor to the change in LULC (Sleeter et al., 2013).

2.6. Predicting future coastal LULC change

In the IDRISI Terrset v-18.31 program, the CA-Markov model is used to assess spatial-temporal LULC change (Ghosh et al., 2017; Islam and Ahmed, 2012). The CA-Markov model combines the Markov chain and cellular automata to predict the trends and patterns of LULC change over time, give a more precise knowledge of the drivers of change, and create a future map of LULC change to enable the creation of conservation policies (Pirasteh et al., 2021). Additionally, this model is frequently used to map the dynamics of forest cover, the extension of developed lands, plant growth, and watershed management modeling.

To predict future coastal LULC changes for the study area, the following steps are taken: (a) coastal LULC maps for the years 2000 and 2020 were used to obtain the transition probabilities image; (b) Considering the CA-Markov model approach, the coastal LULC map for 2020 was simulated using the transition probabilities; (c) transition suitability image was computed using constraints and factors in the multicriteria evaluation (MCE) module; (d) Finally, the coastal LULC changes for the years 2040 and 2060 are predicted using the transition probabilities images, base map, and transition suitability image (Fig. 7). We adopted the equations used by Islam and Ahmed (2012) and Li et al. (2015), to predict the coastal LULC change in the study area.

2.7. Future impact of SLR on coastal land use and habitat quality

The Sea Level Affecting Marshes Model (SLAMM) v-6.7 predicts the main processes involving wetland conversions and coastal LULC change within short, medium, and long-term SLR scenarios. SLAMM predicts when and where coastal lands will possibly experience a change in inundation as a result of SLR. Under accelerated SLR scenarios, the coastal LULCs are predicted, and the results are presented in tabular and Geographic Information System (GIS) formats. According to a set of LULC codes (Suppl T1) in SLAMM, each coastal LULC class in the study region is categorized (Clough et al., 2016). Digital elevation model (DEM), intertidal slope, and SLR scenarios were some of the model inputs used in this work, which also included the SLAMM category described in SLAMM 6.7's technical documentation (Clough et al., 2016). The spatial interpolation feature in ArcGIS 10.5 was used to create the DEM and intertidal slope at a resolution of 15 m. The ArcGIS 10.5 data conversion tool was then used to convert the layer of DEM and intertidal slope from raster data format to ASCII text format.

This study used two scenarios to project the effects of SLR on land use and habitat quality. We merged the local SLR data (0.1 m), measured by Lopes et al. (2022) between 2008 and 2020 in the NC-GB, used as a baseline with the future high-emissions Representative Concentration Pathway (RCP8.5) for the years 2040–2100. Following RCP2.6, RCP4.5, and RCP6.0; the RCP8.5 is the most recent scenario that predicts a global mean SLR of 0.52–0.98 m by 2100. The projections are made for three time periods: the short term (2020–2040), the medium term (2020–2060), and the long term (2020–2080).

3. Results

3.1. Classification's accuracy assessment

Between 2000 and 2020, the NC-GB coastal LULC's overall accuracy was assessed using the Kappa coefficient. A Kappa value larger than 0.5 can be considered suitable. While >0.79 denotes exceptional quality, and one of 0.59 or less indicates moderate to inadequate quality (Cohen, 1968). The 2020 coastal LULC was accurately achieved with 88%. So it was clear that the 2020 classified image was obtained with good results. Compared to the overall accuracy score of 87% for the 2000 classified image (see Suppl. T2 for more details).

3.2. Quantified coastal LULC change

Fig. 7 shows the coastal LULC change maps for the years 2000 and 2020. Table 3 displays the statistical areas for the various coastal LULC classifications. The findings demonstrate that the tidal flat area underwent significant changes between 2000 and 2020, rising from 6.23% to 8.43%. Both developed lands and coastal mangrove have decreased as a result of the considerable tidal flat change during the previous two decades (Fig. 2). In 2000, there were 10.01% of land areas that were developed; by 2020, that number had dropped to 9.45%. Similar declines were seen in mangrove, which went from 18.00% to 17.14% respectively. This decline in developed land and mangroves is related to the study area's increased tidal flat aggravated by SLR, which rose 8.79 mm/y (Lopes et al., 2022). Between 2000 and 2020, the mixed forest increased from 14.39% to 15.02% (Table 2). This growth is related to the recent three decades' large-scale monoculture production of cashew nuts (del-Toro and López, 2019). According to IBAP (2019) most recent study, large-scale cashew nut monoculture activities in Guinea-Bissau are lowering the amount of Savana and barren areas. The change of the coastal LULC analysis was through evaluation of gains or losses, and net change experienced by different classes using change analysis in LCM of Idrissi TerrSet software. Table 2 and Fig. 2 show the dynamic of spatial-temporal changes of different classes between the years 2000 and 2020.

The gains and losses of different coastal LULC classes are displayed in Fig. 2 and Table 2. Major coastal LULC gains involved the expansion of tidal flat and mixed-forest; and the main losses are the reduction in developed land, mangrove and open water. From 2000 to 2020, tidal flat gained 100.61 km^2 and loss −42.68 km^2, with a net gain of 57.93 km^2 (Fig. 2 and Suppl. F2). Developed land lost −75.58 km^2 and gained 37.17 km^2, with a net loss of −38.41 km^2. The sand beach slightly lost −2.71 km^2 and gained 2.26 km^2 with a net loss of −0.45 km^2. Mixed-forest, increased with a net gain of 48.61 km^2 and loss of −22.71 km^2,

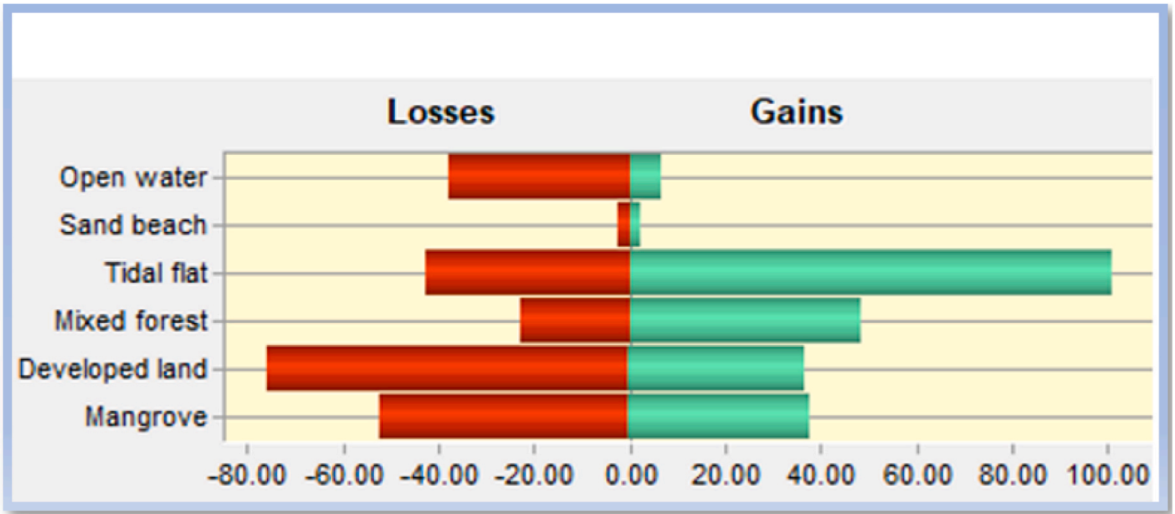

Fig. 2. Gains and losses by each class in the northwestern coastline of Guinea-Bissau from 2000 to 2020.

Table 2
Statistics area of the coastal LULC change classes for the years 2000–2020 in the Northwestern Coastline of Guinea-Bissau.

Coastal LULC	Area (Km^2/%)				Change area (Km^2)		
	2000		2020		2000–2020		2000–2020
	Km^2	%	Km^2	%	Loss (Km^2)	Gain (Km^2)	Net change (Km^2)
Mangrove	443.29	18.00	429.39	17.14	−52.37	38.35	−14.02
Developed land	250.72	10.01	212.12	9.45	−75.58	37.17	−38.41
Mixed forest	343.91	14.39	369.86	15.02	−22.71	48.61	25.90
Tidal flat	148.07	6.23	206.25	8.43	−42.68	100.61	57.93
Sand beach	3.19	0.33	2.64	0.17	−2.71	2.26	−0.45
Open water	1277.79	52.19	1246.72	51.28	−37.63	6.68	−30.95
Total area	**2466.98**	**100**	**2466.98**	**100**	=	=	=

Table 3
Statistics area of the coastal LULC change classes for the predicted years 2040–2060 in the northwestern coastline of Guinea-Bissau.

Coastal LULC	Area (Km^2/%)				Change area (Km^2)		
	2040		2060		2040–2060		2040–2060
	Km^2	%	Km^2	%	Loss (Km^2)	Gain (Km^2)	Net change (Km^2)
Mangrove	435.39	18.34	436.84	17.10	−3.98	5.15	1.17
Developed land	185.64	8.23	170.31	9.39	−17.46	2.10	−15.36
Mixed forest	386.33	16.17	397.55	15.10	−0.85	12.18	11.33
Tidal flat	241.80	8.03	264.48	10.00	−5.32	27.94	22.62
Sand beach	2.64	0.40	2.68	0.28	−0.42	0.44	0.02
Open water	1216.71	49.01	1196.67	51.13	−20.36	0.58	−19.78
Total area	**2468.52**	**100**	**2468.52**	**100**	=	=	=

with net gain of 25.90 km^2.

The contribution to the net change of the all classes is presented in Suppl. F3. The net loss of mangroves has been caused by four coastal LULC classes, including open water, mixed-forest, tidal flats, and developed land (Suppl. F3). The biggest contributions were from tidal flat of roughly −8.30 km^2 followed by developed land −3.20 km^2 and open water −2.00 km^2, respectively. Mangroves made a negligible contribution to the net gain, with a value of under 1.00 km^2. A total of two coastal LULCs contributed to the developed land's net loss. The largest contributions came from the tidal flat with −15.89 km^2 and the mixed forest with roughly −25.78 km^2. Three coastal LULC made contributions to the net gain by tidal flat such as, mangroves (8.30 km^2), developed land (15.89 km^2), and open water (32.6 km^2). See Suppl. F3 for more details.

3.3. *Driving forces of coastal LULC change*

3.3.1. *Socioeconomic drivers*

The socioeconomic influence on coastal LULC in this study refers to changes in ecosystems and habitat quality driven on either directly or indirectly by human pressure (Aghdam et al., 2016). Reduced habitat quality is a result of rising human population and increased deforestation. Reversing the situation requires conservation, the protection of ecosystems and the creatures that live there. In general, the conversion of mangroves, mixed-forest, and tidal flats into agricultural land and infrastructure projects had a negative impact on habitat quality.

The most substantial impact on habitat quality was caused by converting tidal flats into agricultural land, with a value of −0.91. The next most prevalent conversion was from mixed-forest to cultivated land, thus, the conversion of mangroves into agricultural area was the least dominant (see Fig. 3). The conversion of mixed-forest into infrastructural area had the strongest influence on habitat quality, followed by tidal flat, and mangroves which was the least impacted by infrastructural actions (see Fig. 3). The conversion of agricultural land into habitat has a positive impact. Contrarily, the conversion of agricultural land had a positive impact on the habitat quality of mangroves, mixed-forests, and tidal flats. Additionally, the conversion of infrastructure sites had a positive impact on the habitat quality of mangroves, mixed forests, and tidal flats. Illustrates both negative and positive habitat quality conversions, focusing on agricultural and infrastructure sectors.

3.3.2. Coastal hazards drivers

The term "coastal hazards" in this assessment refers to hydrological phenomena such coastal erosion and accretion. Particularly, sea-level rise and storm-surges have an influence on these phenomena (Szlafsztein and Sterr, 2007). They have the potential of impacting the coastal population, infrastructures, ecosystem and biodiversity (Boruff et al., 2005). The rate of temporal change in coastal erosion and accretion was estimated between 2000 and 2020, taking into account sea-level rise, one of the main drivers affecting the quality of coastal habitat. The study discovered that there were changes in all of the study area's coastline (Fig. 4). The net shoreline measurement (NSM) revealed a maximum erosion of 450 m and a minimum of 100 m, as well as a maximum accretion of about 400 m and a minimum of 90 m over a period of 20 years. These general trends of erosion and accretion vary according to the coastal LULC characteristics (sea Fig. 4). The rates of shoreline variations, measured by the NSM over the two decades, indicated that the shoreline change is potentially subjected to slight aggradation to coastal habitat quality.

3.3.3. DEM and slope implication

The variables that determine changes were based on spatial analyses integrated into the model as static or dynamic elements (Leta et al., 2021). DEM and Slope were chosen in this study to analyze their contribution to the changes of coastal LULC. The change in coastal LULC is not sufficiently explained by Cramer's V-value. Instead, it is a simpler technique that may be used to understand the importance of a single variable in determining the changes (Leta et al., 2021). In circumstances where Cramer's V is low, it is typically advised that the probability of evidence result is regarded as being good (Fig. 5). In this study, the difference between tidal flats and all other land classes is quantified. We found the Cramer's V-values of DEM is useful variable of transitions. Low Cramer's V-values for the slope variable indicate that the influence on changes in coastal LULC is only moderately critical in the study area (see Fig. 5). The DEM is the prominent contributors of coastal LULC changes in the study area rather than slope. These variables have contributed to the significant extent of sea-water to tidal flat, tidal flat to developed land, and mangrove to mixed-forest. According to Fig. 5, a large fraction of the study area had low elevation and a flat slope, which could facilitate the quick and easy penetration of ocean water into the coastal LULC (Lopes et al., 2022).

3.4. Predicted future coastal LULC change

The base map 2000–2020 has been used to predict the future coastal LULC change for the years 2040–2060 (Fig. 6). Future changes in coastal LULC were examined for the years 2040 and 2060 using the transition probability matrix. The Markov chain provides the spatial distribution and amount of change, which are the two elements of the coastal LULC prediction in LCM (Leta et al., 2021). Fig. 6 shows the coastal LULC changes in the NC-GB derived from the LCM data. Table 3 displays the statistic area, percentage, gain or loss, and net change.

Between 2000 and 2060, significant coastal LULC change was observed. Tidal flats have been driving LULC change along the coast. The results show that, it will increase from 148.07 km^2 in 2000 to 264.48 km^2 by 2060, with total net change of 80.55 km^2 (Table 3 and Suppl. F4). These changes were mostly driven on by the sea-level rise reported in the earlier section 3.3.2 analysis in this study. Similar to mixed-forest, which will grow from 343.91 km^2 in 2000 to 397.55 km^2 in 2060, there will be a net change of 37.23 km^2. Because cashew nuts are one of the country's primary strategic economic products, their growing tendency has been a major factor in the progressive expansion of mixed-forests (IBAP, 2019). The study observed that developed land will decrease from 250.72 km^2 in 2000 to 170.31 km^2 by 2060 with total

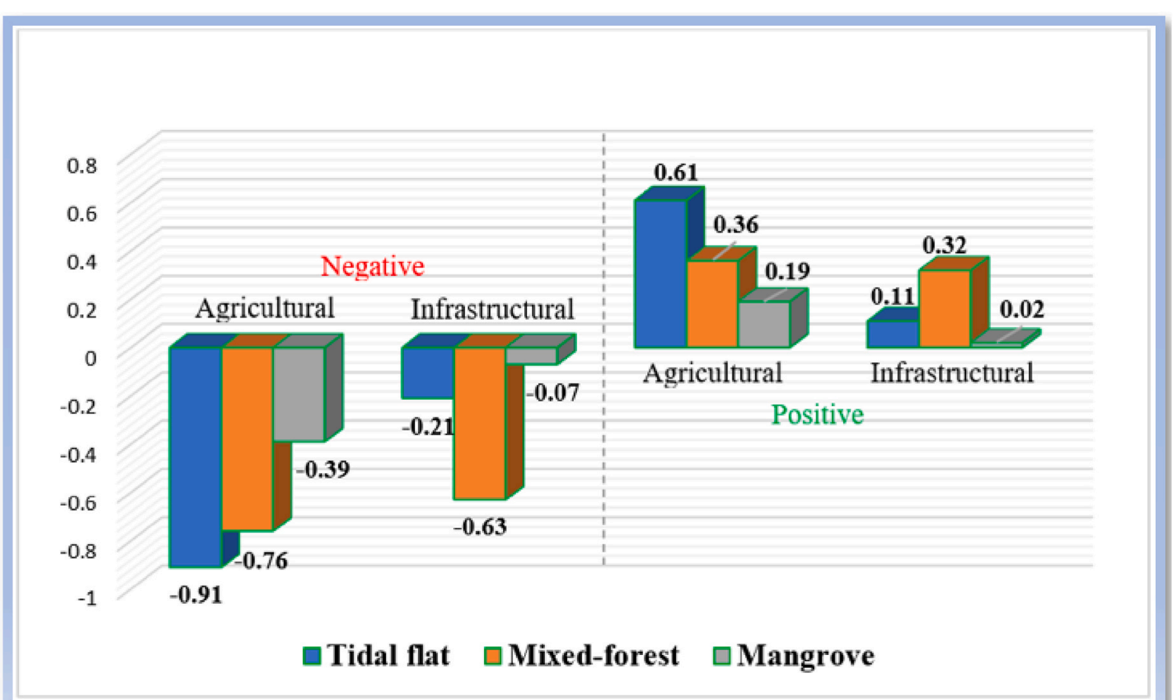

Fig. 3. Negative and positive conversions influenced by socioeconomic drivers (agricultural and infrastructural activities).

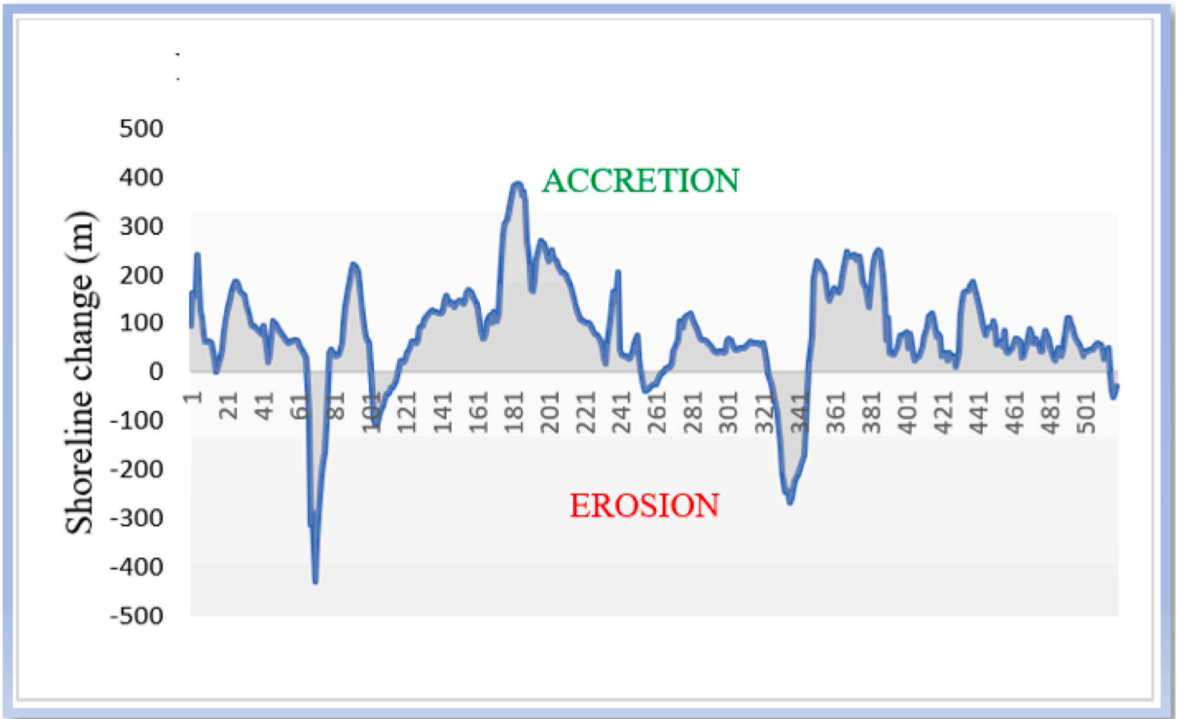

Fig. 4. Net shoreline change (Erosion and Accretion) based on NSM values in (m) between 2000 and 2020.

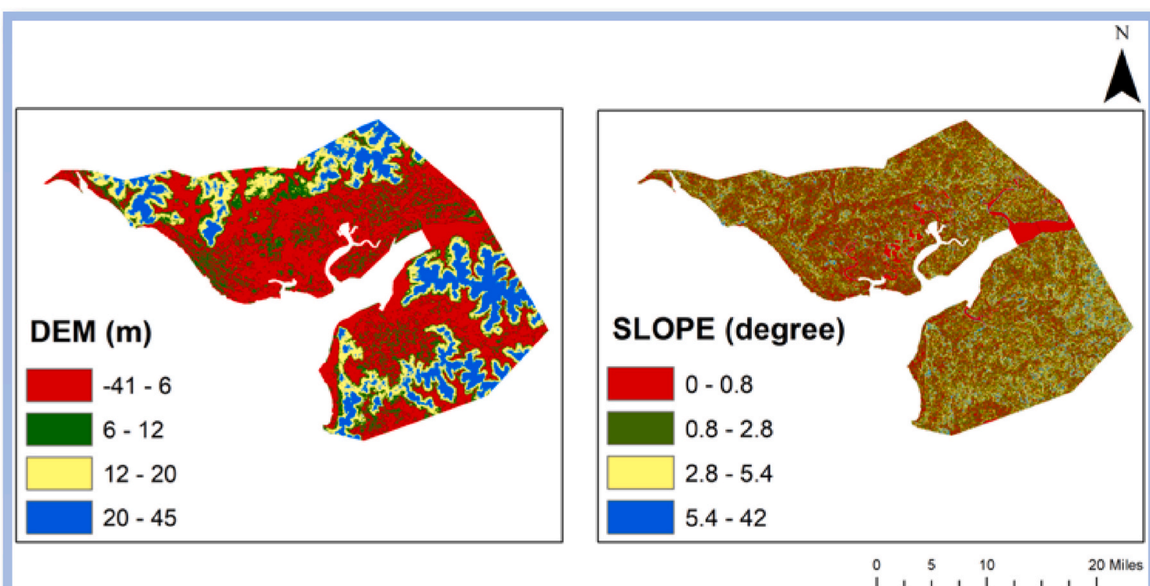

Cramer's V values and p-value for each of the explanatory variables

Driver variables	Cramer's V values	p-value
DEM	0.1435	0.0000
SLOPE	0.0032	0.0000

Fig. 5. DEM and slope variables associated with Cramer's v values and p-value.

net change of −53.77 km^2 (Table 3 and Suppl. F4). This progressive decline has primarily been driven on by unplanned infrastructures in the study area that have been impacted by SLR and tidal flat (del-Toro and López, 2019). The findings also indicate that by 2060, mangrove and sand beaches will only notice minor changes, as seen in Table 3 and Suppl. F4. Mangroves have been chosen as a priority for protection and conservation because of the study area's high coastal vulnerability (IBAP, 2019; Lopes et al., 2022). Tidal flat and mixed-forest expansion

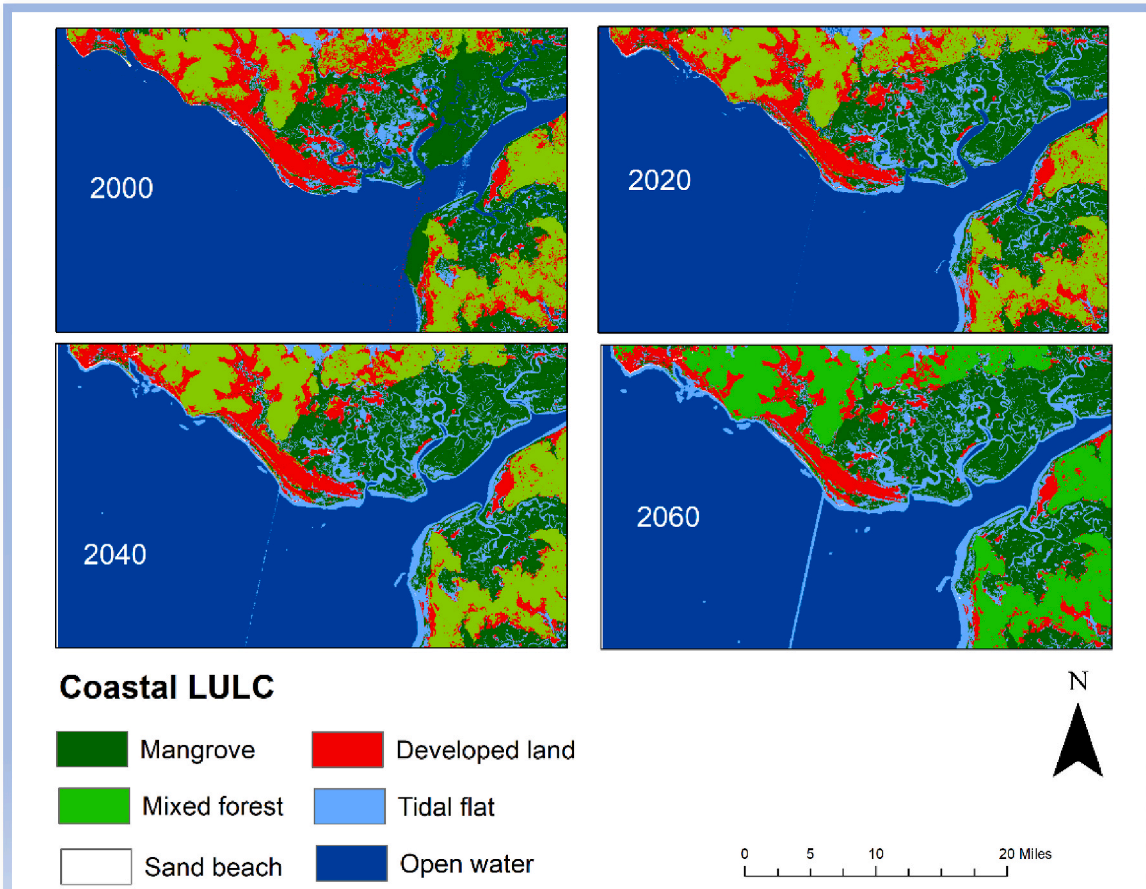

Fig. 6. The future coastal LULC change prediction in the northwestern coastline of Guinea-Bissau for year 2040 and 2060 based on the years 2000–2020.

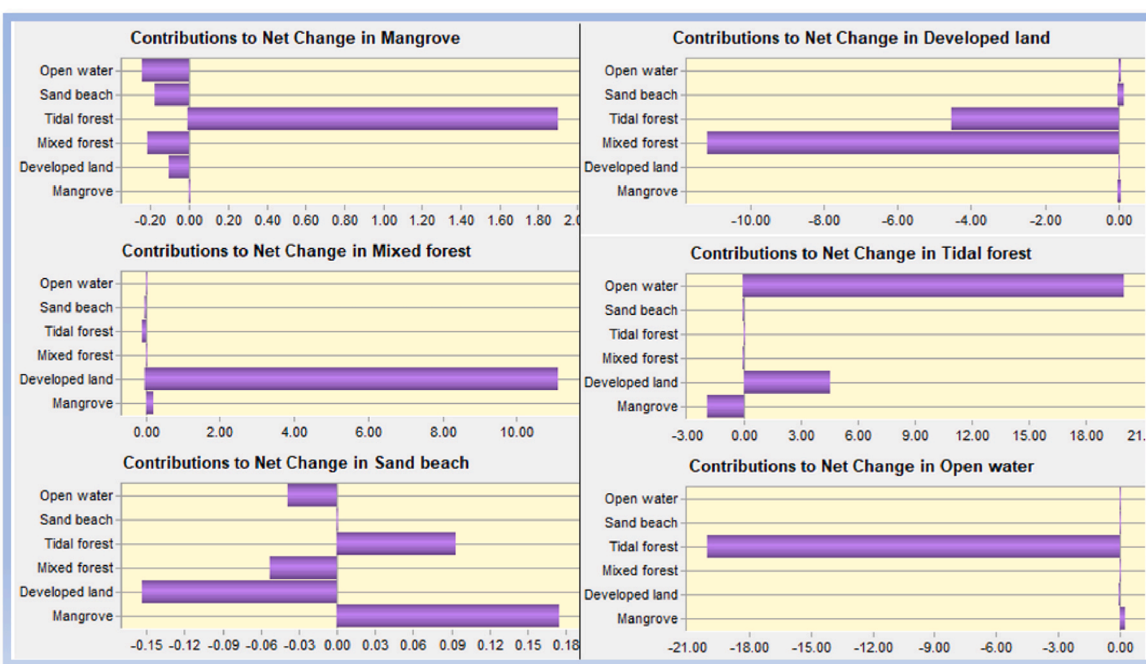

Fig. 7. Contribution to net change experienced by mangrove, developed land, tidal flat, mixed-forest, sand beach and open water in the northwestern coastline of Guinea-Bissau from 2020 to 2060.

will be the major coastal LULC gain from 2040 to 2060, while open water and developed land were the main losses. Tidal flats will have the greatest gain between 2040 and 2060, followed by mixed forest and mangrove (see Suppl. F5). Open water and developed land, on the other hand, will see a record loss in the study area. The sand beach will slightly experience both loss and gain (see Suppl. F5).

Only one coastal LULC class will contribute to the net change, which will result in a benefit for mangroves and tidal flats (see Fig. 7 and Suppl. T3). Open ocean, mixed-forest, sand beaches, and developed land, will each make a negligible contribution to the net loss that mangroves will suffer. Two coastal LULCs will make contributions to the net loss of developed land, including mixed-forests with a large contribution and tidal flats with a relative contribution. A small portion of area will be gained to sand beach. Tidal flat gains will come from two coastal LULC, such as open water and a relative amount of developed land (See Fig. 7 and Suppl. T3). The dynamic increase and decline of coastal LULC from 2000 to 2060 in the study area are shown in Suppl. F6 and Suppl. F7. Between 2000 and 2060, there is a trend toward less developed land, and this trend is environmentally friendly because it eases pressure on the coastal ecosystem and biodiversity. Contrary to the trend of less open water, this change will have two major consequences first, less salty water will enter agriculture and aquifers, which will have beneficial economic and social impacts; second, coastal habitats will suffer (environmentally unfriendly).

3.5. Future impact of SLR on the coastal land use and habitat quality

Even if greenhouse gas emissions remain on a relatively modest trajectory in the following decades, the global mean sea level is predicted to rise by at least 0.3 m by the end of 21st century (Gilman et al., 2007). Over the next 60 years, it is predicted that the sea level will rise along the coastline, having a particular impact on the lowlands. SLR along the shoreline will vary depending on the region due to changes in both land and ocean elevation (Ferreira et al., 2014). SLR resulting from RCP8.5 pathways will substantially alter coastal land use and habitat quality in the NC-GB by 2040–2080 (sea Fig. 8 and Table 4). Suppl. F8summarizes the projection results of the short-, medium-, and long-term impacts of SLR on coastal land use and habitat quality under the high emission scenario of RCP8.5 for the years 2040, 2060, and 2080. The findings of Suppl. F8 are based on local SLR data obtained by Lopes et al. (2022) from 2008 to 2020 in the study area, and are intended to serve as a baseline for future projections of the impact on coastal land use and habitat quality. The results show that if no action is made to protect the coastline in such a coastal area, sea level will rise dramatically. Within the RCPs scenarios, these results are fairly similar to the global ones published by the IPCC (2013).

3.5.1. Short-term SLR impact (2020–2040)

Fig. 8b presents the results of the SLAMM projections of the short-term SLR impact on coastal land use and habitat quality under the local and RCP8.5 scenarios. Table 4 provides a summary of the statistic area, percentage of coastal land use, and habitat quality that will be

Table 4
The total area and percentage of the coastal LULC that will be impacted over the short, medium, and long-term series in the study area.

SLAMM Category	2020–2040		2020–2060		2020–2080	
	km^2	%	km^2	%	km^2	%
Mangrove	1.15	15	3.26	20	5.81	23
Developed land	5.58	74	10.73	65	16.19	64
Mixed forest	0.76	10	2.07	13	3.01	12
Tidal flat	=	=	=	=	=	=
Sand beach	0.03	0	0.05	0	0.30	1
Open water	=	=	=	=	=	=
Total impacted area	7.52	100	16.56	100	25.31	100

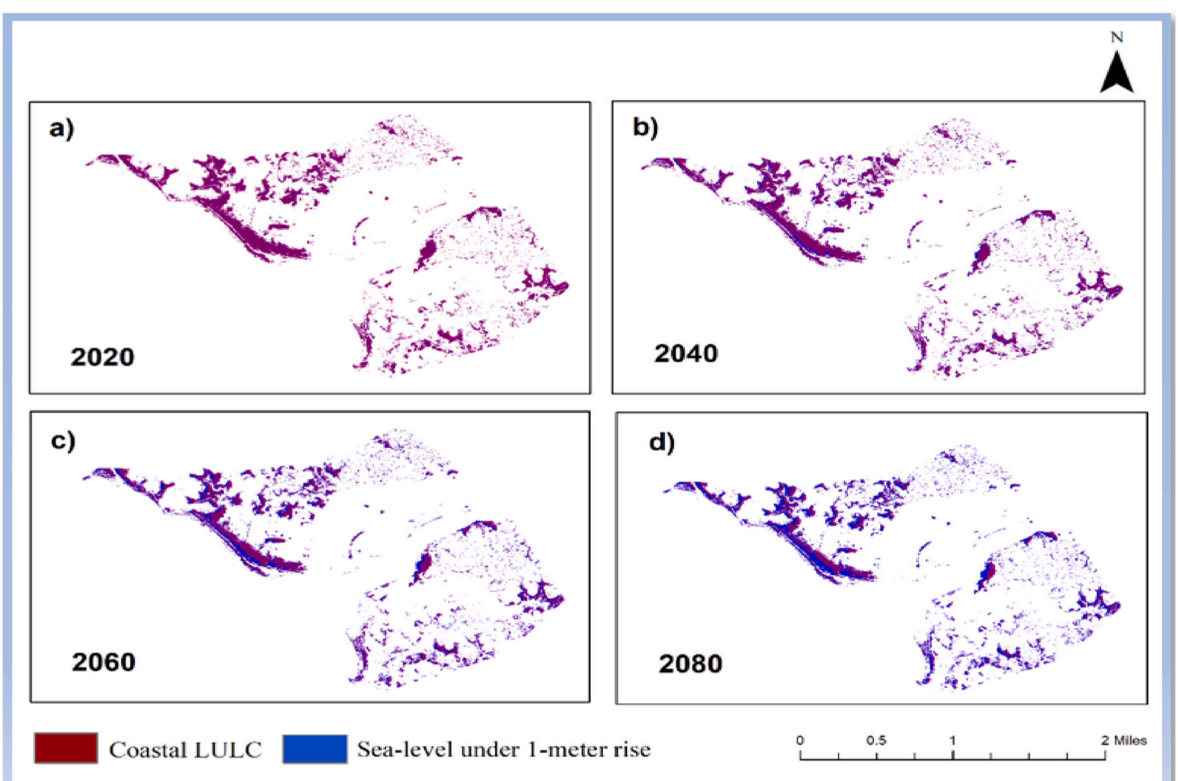

Fig. 8. The projected coastal LULC that will be impacted under the local and RCP8.5 sea-level rise scenarios, without coastal protection in the study area from 2020 to 2080.

impacted over the short-term series. SLAMM results show that by 2040, SLR will have an impact on 7.52 km^2 of the overall coastal land use (Fig. 8a). Developed land will be the most impacted land in the study area with total of 5.60 km^2. The habitat of mangrove and mixed forest will be most impacted with 1.16 km^2 and 0.76 km^2, respectively. The lack of coastline protection in these areas, as well as their lower elevation of less than 5 m above mean sea level and flat slope of around 2–5°, may be the main factors of this impact (Fig. 5). The result of the short-term projection indicates that SLR will not have much impact on mangrove and mixed-forest habitats in the coming two decades.

3.5.2. Medium-term SLR impact (2020–2060)

The SLAMM projection results of medium-term SLR impact on coastal land use and habitat quality under the local data and RCP8.5 scenarios are presented in Fig. 8b. The statistic area and percentage of the coastal land use and habitat quality that will be impacted over the medium-term series are summarized in Table 4. According to SLAMM results, nearly 16.56 km^2 of the total coastal land use will be impacted by SLR by 2060 (Fig. 8c). Developed land will be the leading most impacted land with total approximately 11.73 km^2. The habitat of mangrove and mixed-forest will be the first and second most impacted with 3.26 km^2 and 1.27 km^2, respectively. The absence of coastline protection in these locations is the biggest factor of this impact. The other reasons are related to lower elevation as well and flat slope observed in the study area. The other factors are connected to the study area's flat slope and lower altitude as well (Fig. 5). According to the medium-term prediction, mangrove and mixed forest will have only small impact from SLR, as shown in Fig. 8.

3.5.3. Long-term SLR impact (2020–2080)

In accordance with the local data and RCP8.5 SLR scenarios, the SLAMM projection results of the long-term SLR impact on coastal land use and habitat quality are shown in Fig. 8d. Table 4 summarizes the overall area and the percentage of the coastal LULC that will be impacted during the long-term series. Results from the SLAMM project that by 2080, sea level rise will have an impact on almost 25.31 km^2 of the entire coastal land usage (Fig. 8d). Developed land will continuously be the most impacted land use with approximately 16.19 km^2. Mangrove and mixed-forest will be the second and third most impacted with 5.81 km^2 and 3.01 km^2, respectively. The main factors of the impact have to do with no coastal protection, the low coastal elevation, and flat slope observed in these areas (Fig. 5). The long-term projection results indicate that SLR will have huge impact on mangrove and mixed-forest as can be observed in Fig. 8.

4. Discussion

4.1. Recommendation for coastal protection

The coastline of Guinea-Bissau, which extends 150 km into the interior of the country, makes up about 65% of the national territory (Seatemperatureinfo, 2021). This coastal country is classified in two different zones: the northwest zone which comprises the Region of Cacheu (study area), Biombo, and Autonomous Region of Bissau (the Capital); and the southwest which includes the Region of Quinara, Tombali and Bolama Bijagós Archipelago. As a result, there is a complex link between socioeconomic activity, sea level rise, and coastal LULC (Lopes et al., 2022). The first administration in Guinea-Bissau was established in 1974 (Patrick, 1981), and since then, there has been a significant increase in the use of land for urbanization and food production. Such activities, especially in the northwestern coastal zones, have slowly contributed to the coastal LULC change.

The results of this study indicate that the change in mixed-forest is favorable because cashew nut farms became a critical economic product after the country gained independence in 1973 (Patrick, 1981), accounting for more than 90% of total exports and 20% of GDP, (Mendy et al., 2013). Due to this product's economic importance, a significant portion of the rural population focused on its marketing and cultivation. Plantations for cashew nuts occupy more than 70% of the forest area, mostly in the northwest (FAO, 2019). Between 2000 and 2020, cashew nut cultivation areas were estimated at 253,000 ha, with an annual production of 140,000 tons of raw cashew nut (FAO, 2019). However, since then, annual production has climbed, and by 2020, exports have exceeded 180,004 tons, putting the nation the seventh-largest producer in the world and fourth in Africa, behind Ivory Coast, Benin, and Tanzania (FAO, 2019). Because of the high percentage of poverty in rural regions, natural resources are being used carelessly, which has resulted in the destruction of timber forests for trade and the alteration of ecosystems for the practice of rice farming. In Guinea-Bissau, 79% of the workforce is employed in the production of rice, which is typically grown in both the drier savanna region and the marshy coastal regions. Rice production has fluctuated substantially in recent years, from an increase of 50,000 tons by 2000 to approximately 187,000 tons in 2019 corresponding to 26.73% of the increase (Knoema, 2019). These socio-economic issues, namely the conversion of tidal flats and mixed-forest into agricultural areas, have considerably contributed to the decline of coastal habitats.

The findings of this study predict that mixed-forest will grow during the next 40 years. SLR is a major factor in the rise of tidal flat, and these rises have had an adverse effect during the past two decades. Tripathi et al. (2018), provided evidence to support the claim that tectonic compaction and SLR related to storm surge have a significant impact on coastal LULC charges. Low-elevation and flat-sloped areas are particularly susceptible to SLR effects. The tidal flat is moved and settled by hydrodynamic processes based on directions relative to sea level. The study area experienced an annual rise in high tide of more than 2.8 m (Hidrografico.pt, 2021) and an SLR rate of 8.79 mm/year (Lopes et al., 2022), that is significantly greater than the predicted 3.1 mm/year for the global average (Bhuiyan et al., 2012). This has caused the tidal flat to gradually rise between 2000 and 2020, and by 2060, there will be comparable changes. A significant factor in these changes will be the flat coastline slope of less than 2° and lower elevation of less than 1 m below mean sea level seen in much of the study are. Developed lands, such as paddy fields, horticulture, build-up, and dry lands, have been affected by the expanded tidal flat as a result of rapid SLR. This impact is due to the influx of saline water onto agricultural lands and the relocation of coastal populations to the inland areas. Between 2000 and 2020, mangroves only slightly changed, but during that time, restoration and conservation efforts in the NC-GB made significant advancements in wetlands, which allowed for a significant expansion of the mangrove ecosystem (IBAP, 2019; IUNC, 2018). IBAP (2019), estimates that the mangroves in Guinea-Bissau cover about 326,000 ha, or 9% of the country's land area. The study's findings showed that, the impact of accelerated SLR poses a serious risk to developed land, mixed-forest, and mangroves especially under the current and RCP8.5 scenarios. The study area is largely exposed to the Atlantic Ocean and highly vulnerable to SLR; without adequate protection, the potential decrease of coastal LULC and habitat quality in the NC-GB is unavoidable in the short-, medium- and long-term scenarios. To reduce the potential impacts of tidal flats related to SLR in the coastal LULC in the NC-GB, protective measures should be taken.

➢ Properly restoring wetlands and native woodland patches can help to restore the consistency of the coastal ecosystem, which is essential for coastal protection (Berlanga-Robles and Ruiiz-Luna, 2002).
➢ In order to reduce coastal flooding and safeguard low-lying built areas in the NC-GB, landward boundaries can be fixed as seawalls or setback zones can be implemented by creating dykes (Harman et al., 2015). These seawalls could stop the mangrove environment from moving upward and prevent the eventual loss of this ecosystem due to SLR or tidal flats.

- ➢ To stop seawater from polluting or invading agricultural and community lands, buffers can be built along tidal waterways.
- ➢ By limiting the force of tidal advance, soft technologies like sand barriers or geotextile bags filled with sand beaches can be an effective measure to safeguard this area.

5. Conclusion

This study is the first-ever to predict the dynamics of coastal LULC change and the impact of SLR on coastal land use and habitat quality in the NC-GB. The goal of the study was to comprehend the changes and their impact on past and future trends in LULC change between the years 2000 and 2060. The combined techniques employed for data preprocessing, maximum likelihood classification, and accuracy assessment included remote sensing and GIS-related techniques; integrated Land Change Modeler (LCM), Habitat Quality Model (HQM), and Digital Shoreline Analysis System (DSAS) to quantify the temporal change and driving forces of the coastal LULC between 2000 and 2020; combined CA-Markov Model with Sea Level Affecting Marshes Model (SLAMM) and merged the local study area's SLR data with future representative concentration pathway (RCP8.5) scenarios to predict future coastal LULC change and associated sea-level rise (SLR) impact on the coastal land use and habitat quality in short-, medium- and long-term. The conclusions drawn from the results were as follows.

Decisions about coastal LULC changes are based on multitemporal remote sensing data, which also provide the information needed to monitor coastal LULC changes. The maximum likelihood supervised classification performed successfully and accurately with the 15 m resolution remote sensing data that was used. The NC-GB has undergone significant coastal LULC changes over the past two decades (2000–2020) driven on by socioeconomic activity and SLR actions. Tidal flats, whose change was mostly driven by open water (sea level), saw a net gain of 57.93 km^2, whereas mixed-forest, whose gain was driven by developed land, saw a net change of 25.90 km^2. The study also noted the disappearance of two major coastal LULCs, including developed land driven by mixed-forest and tidal flat, which lost a total of -75.58 km^2, and open water, whose change was mostly driven by tidal flat, which lost a net of -37.63 km^2. In terms of gain and loss, mangrove and sand beaches showed little changes. A cumulative gain of 80.55 km^2 in tidal flat area and a loss of -53.77 km^2 in developed land are the two primaries coastal LULCs that will experience significant changes between 2020 and 2060. From 2020 to 2080, developed land will be the most impacted coastal LULC with 64%, followed by mangrove with 23%, and mixed forest the last with 12%.

The study came to the conclusion that the conversion of mangroves, mixed-forest, and tidal flats into agricultural and infrastructure areas were the primary drivers influencing coastal LULC and habitat quality change in the NC-GB. The coastal erosion and accretion, which caused the loss of significant ecosystems in the coastlines, were the other cause of the changes. Over a 20-year period, the studied area experienced maximum erosion of 450 m and accretion of about 400 m. The study came to the further conclusion that the study area's low coastline elevation of -1 m and flat slope of less than 2° in most of the study area have contributed to coastal LULC and habitat quality change. The services provided by the coastal ecosystem, including, the socioeconomic development, and food security will all be put in danger by these unprecedented and alarming changes. However, coastal managers and policymakers need to move quickly to support regional sustainable development.

Credit author statement

All authors reviewed the final manuscript. Namir Domingos Raimundo Lopes: formulated the ideas and research aims, developed the methods, analyzed the data, and wrote the manuscript. Tianxin Li, and Rui M. Sa: equally contributed in research planning, manuscript reviewing and fund acquisition. Peng Zhang: reviewed the manuscript and fund acquisition. Nametso Matomela and Harrison Odion Ikhumhen: equally provided technical comments.

Declaration of competing interest

The authors declare that they have no known competing financial interests or personal relationships that could have appeared to influence the work reported in this paper.

Data availability

The authors do not have permission to share data.

Acknowledgements

This study was supported by Chinese National Key Research and Development Plan (2018YFC1903206), and Malmon (European Union funded project) "Mangroves, Mangrove rice and Mangrove people (FOOD/2019/412–700).

Appendix A. Supplementary data

Supplementary data to this article can be found online at https://doi.org/10.1016/j.jenvman.2022.116804.

References

Abdullah, S., Adnan, M.S.G., Barua, D., Murshed, Md-M., Kabir, Z., Chowdhury, M.B.H., Hassan, Q.K., Dewan, A., 2022. Urban green and blue space changes: a spatiotemporal evaluation of impacts on ecosystem service value in Bangladesh. Ecol. Inf. 70, 101730 https://doi.org/10.1016/j.ecoinf.2022.101730.

Abijith, D., Saravanan, S., 2021. Assessment of land use and land cover change detection and prediction using remote sensing and CA Markov in the northern coastal districts of Tamil nadu, India. Mapping Intimacies 1–26. https://doi.org/10.21203/rs.3.rs-576976/v1.

Addo, K.A., 2010. Urban and peri-urban agriculture in developing countries studied using remote sensing and in situ methods. Rem. Sens. 2, 497–513. https://doi.org/10.3390/rs2020497.

Aghdam, I.N., Varzandeh, M.H.M., Pradhan, B., 2016. Landslide susceptibility mapping using an ensemble statistical index (Wi) and adaptive neuro-fuzzy inference system (ANFIS) model at Alborz Mountains (Iran). Environ. Earth Sci. 75, 1–20. https://doi.org/10.1007/s12665-015-5233-6.

Al-sharif, A.A.A., Pradhan, B., 2014. Monitoring and predicting land use change in Tripoli Metropolitan City using an integrated Markov chain and cellular automata models in GIS. Arabian J. Geosci. 7, 4291–4301. https://doi.org/10.1007/s12517-013-1119-7.

Al-Tahir, R., Asim Ali, A., 2004. Assessing land cover changes in the coastal zone using aerial photography. Land Inf. Sci. 64, 107–112. file:///C:/Users/Lopes/Desktop/SaLIS_AssessingLCChangesintheCoastalZone-Al_Tahir.pdf.

Alam, A., Bhat, M.S., Maheen, M., 2019. Using Landsat satellite data for assessing the land use and land cover change in Kashmir valley. Geojournal 85, 1529–1543. https://doi.org/10.1007/s10708-019-10037-x.

Xiaowei, C., Huanga, X., Wang, W., Zhao, R., Zhang, M., Wua, C., 2015. Land use, total carbon emissions change and low carbon land management in Coastal Jiangsu, China. J. Clean. Prod. 103, 77–86. https://doi.org/10.1016/j.jclepro.2014.03.046s.

Baig, M.F., Mustafa, M.R.U., Baig, I., Takaijudin, H.B., Zeshan, M.T., 2022. Assessment of land use land cover changes and future predictions using CA-ANN simulation for selangor, Malaysia. Water 14, 402. https://doi.org/10.3390/w14030402.

Belward, A.S., Skøien, J.O., 2015. Who launched what, when and why; trends in global land-cover observation capacity from civilian earth observation satellites. ISPRS J. Photogrammetry Remote Sens. 103, 115–128. https://doi.org/10.1016/j.isprsjprs.2014.03.009.

Berlanga-Robles, C.A., Ruiz-Luna, A., 2002. Land use mapping and change detection in the coastal zone of northwest Mexico using remote sensing techniques. J. Coast Res. 18, 514–522. https://www.jstor.org/stable/4299098.

Bhuiyan, Md, J, A.N., Dutta, D., 2012. Analysis of flood vulnerability and assessment of the impacts in coastal zones of Bangladesh due to potential sea-level rise. Nat. Hazards 61, 729–743. https://doi.org/10.1007/s11069-011-0059-3.

Boruff, B., Emrich, C., Cutter, S.L., 2005. Erosion hazard vulnerability of US coastal counties. J. Coast Res. 215, 932–942. https://doi.org/10.2112/04-0172.1.

Cheruto, M., Kauti Kauti, M.K., Kisangau, P.D., Kariuki, P.C., 2016. Assessment of land use and land cover change using GIS and remote sensing techniques: a case study of makueni county, Kenya. J. Remote Sens. GIS 5, 1000175. https://doi.org/10.4172/2469-4134.1000175.

Clough, J.S., Park, R.A., Fuller, R., 2016. SLAMM 6 Beta Technical Documentation Release 6.0.1 Beta. http://warrenpinnacle.com/prof/SLAMM6/SLAMM_6.7_Technical_Documentation.pdf.
Cohen, J., 1968. Nominal scale agreement with provision for scaled disagreement or partial credit. Psychol. Bull. 70, 213–220. https://doi.org/10.1016/j.catena.2021.105307.
Congalton, R.G., Green, K., 2019, third ed.. Assessing the Accuracy of Remotely Sensed Data Principles and Practices. CRC Press https://popularnetlibrary.blogspot.com/book59.php?asin=1498776663.
Craft, C., Clough, J., Ehman, J., Joye, S., Park, R., Pennings, S., Guo, H., Machmuller, M., 2009. Forecasting the effects of accelerated sea-level rise on tidal marsh ecosystem services. Res. Commun. 7, 73–78. https://doi.org/10.1890/070219.
del-Toro, E.M.G., López, M.I.M., 2019. Changes in land cover in cacheu river mangroves natural park, Guinea-bissau: the need for a more sustainable management. Sustainability 11, 6247. https://doi.org/10.3390/su11226247.
Djouder, F., Boutiba, M., 2017. Vulnerability assessment of coastal areas to sea level rise from the physical and socioeconomic parameters: case of the Gulf Coast of Bejaia, Algeria. Arabian J. Geosci. 10, 1–20. https://doi.org/10.1007/s12517-017-3062-5.
FAO, 2019. Top Countries in Cashew Nuts Production. NationMaster. https://www.nationmaster.com/nmx/ranking/cashew-nuts-production. (Accessed 14 March 2022). accessed.
Ferreira, C., Irish, J., Francisco, O., 2014. Quantifying the potential impact of land cover changes due to sea-level rise on storm surge on lower Texas coast bays. Coast. Eng. 94, 102–111. https://doi.org/10.1016/j.coastaleng.2014.08.011.
Gashaw, T., Bantider, A., Bantider, A., Mahari, A., 2014. Evaluations of land use/land cover changes and land degradation in Dera District, Ethiopia: GIS and Remote Sensing Based Analysis. Int. J. Sci. Res. Environ. Sci. 2, 199–208. https://doi.org/10.12983/ijsres-2014-p0199-0208.
Gashaw, T., Tulu, T., Argaw, M., Worqlul, A.W., 2017. Evalouation and prediction of land use/land cover changes in the Andassa watershed, Blue Nile Basin, Ethiopia. Envi.Syst. Res. 6, 17. https://doi.org/10.1186/s40068-017-0094-5.
Ghosh, P., Mukhopadhyay, A., Chanda, A., Mondal, P., Akhand, A., Mukherjee, S., Nayak, S.K., Ghosh, S., Mitra, D., Ghosh, T., Hazra, S., 2017. Application of Cellular automata and Markov-chain model in geospatial environmental modeling—a review. Remote Sens. Appl.: Society and Environment 5, 64–77. https://doi.org/10.1016/j.rsase.2017.01.005.
Ghoussein, Y., Mhawej, M., Jaffal, A., Fadel, A., El Hourany, R., Faour, G., 2018. Vulnerability assessment of the South-Lebanese coast: a GIS-based approach. Ocean Coast Manag. 158, 56–63. https://doi.org/10.1016/j.ocecoaman.2018.03.028.
Gilman, E., Ellison, J., Coleman, R., 2007. Assessment of mangrove response to projected relative sea-level rise and recent historical reconstruction of shoreline position. Environ. Monit. Assess. 124, 105–130. https://doi.org/10.1007/s10661-006-9212-y.
Hailu, A., Mammo, S., Kidane, M., 2020. Dynamics of land use, land cover change trend and its drivers in jimma geneti district, western Ethiopia. Land Use Pol. 99, 105011 https://doi.org/10.1016/j.landusepol.2020.105011.
Halmy, M.W.A., Gessler, P.E., Hicke, J.A., Salem, B.B., 2015. Land use/land cover change detection and prediction in the north-western coastal desert of Egypt using Markov-CA. Appl. Geogr. 63, 101–112. https://doi.org/10.1016/j.apgeog.2015.06.015.
Han, H., Yang, C., Song, J., 2015. Scenario simulation and the prediction of land use and land cover change in beijing, China. Sustainability-Basel 7, 4260–4279. https://doi.org/10.3390/su7044260.
Hyandye, C., Martz, L.W., 2017. A Markovian and cellular automata land-use change predictive model of the Usangu Catchment. Int. J. Rem. Sens. 38, 64–81. https://doi.org/10.1080/01431161.2016.1259675.
Harman, B.P., Heyenga, S., Taylor, B.M., Fletcher, C.S., 2015. Global lessons for adapting coastal communities to protect against storm surge inundation. J. Coast. Res. 31, 790–801. https://doi.org/10.2112/JCOASTRES-D-13-00095.1.
Hyandye, C., Mandara, G.C., Safari, J., 2015. GIS and logit regression model applications in land use/land cover change and Distri_bution in usangu catchment. Am. J. Rem. Sens. 3, 6–16. https://doi.org/10.11648/j.ajrs.20150301.12.
IBAP, 2019. Instituto da Biodiversidade e das Áreas Protegidas. IBAP. http://ibapgbissau.org/IBAP/Apresentacao. (Accessed 10 May 2021). Accessed on.
IPCC, 2007. Climate Change 2007 Synthesis Report. https://research.monash.edu/en/publications/climate-change-2007-synthesis-report.
IPCC, 2013. The Physical Science Basis. Contribution of Working Group I to the Fifth Assessment Report of the Intergovernmental Panel on Climate Change (IPCC). https://www.ipcc.ch/site/assets/uploads/2018/03/WG1AR5_SummaryVolume_FINAL.pdf.
Islam, MdS., Ahmed, R., 2012. Land use change prediction in Dhaka city using GIS aided Markov chain Modelling. J. Life Earth Sci. 6, 81–89. https://doi.org/10.3329/jles.v6i0.9726.
IUNC, 2018. 95th Meeting of the IUCN Council. Jeju (Republic of Korea). https://www.iucn.org/sites/dev/files/decisions_of_the_95th_meeting_of_the_iucn_council_jeju_6-8_october_2018_with_annex_1-22.pdf. (Accessed 10 March 2021). Accessed.
Kindu, M., Schneider, T., Teketay, D., Knoke, T., 2013. Land use/land cover change analysis using object-based classification approach in Munessa-Shashemene landscape of the Ethiopian highlands. Rem. Sens. 5, 2411–2435. https://doi.org/10.3390/rs5052411.
Knoema, 2019. Guinea Bissau - Rice, Paddy Production Quantity. World Data Atlas. https://knoema.com/atlas/Guinea-Bissau/topics/Agriculture/Crops-Production-Quantity-tonnes/Rice-paddy-production. (Accessed 24 April 2020). Accessed.
Latham, J.S., He, C., Alinovi, L., Di-Gregorio, A., Kalensky, Z., 2002. FAO methodologies for land cover classification and mapping. Linking People, Place, and Policy 283–316. https://doi.org/10.1007/978-1-4615-0985-1_13.
Leta, M.K., Demissie, T.A., Tränckner, J., 2021. Modeling and prediction of land use land cover change dynamics based on land change modeler (LCM) in nashe watershed, upper blue nile basin, Ethiopia. Sustainability 13, 3740. https://doi.org/10.3390/su13073740.
Li, S., Meng, X., Ge, Z., Zhang, Li, 2015. Evaluation of the threat from sea-level rise to the mangrove ecosystems in Tieshangang Bay, southern China. Ocean Coast Manag. 109, 1–8. https://doi.org/10.1016/j.ocecoaman.2015.02.006.
Lopes, N.D.R., Li, T., Qian, D., Matomela, N., Sa, R.M., 2022. Factors influencing coastal land cover change and corresponding impact on habitat quality in the North-western Coastline of Guinea-Bissau (NC-GB). Ocean Coast Manag. 224 (1), 106181 https://doi.org/10.1016/j.ocecoaman.2022.106181.
Marfai, M.A., Almohammad, H., Dey, S., Susanto, B., King, L., 2008. Coastal dynamic and shoreline mapping: multi-sources spatial data analysis in Semarang Indonesia. Environ. Monit. Assess. 142, 297–308. https://doi.org/10.1007/s10661-007-9929-2.
Masrur, Arif, Dewan, A., Botje, D., Kiselev, G., Murshed, M.-M., 2022. Dynamics of human presence and flood-exposure risk in close proximity to Bangladesh's river network: an evaluation with multitemporal satellite imagery. Geocarto Int. https://doi.org/10.1080/10106049.2022.2093410.
Matlhodi, B., Kenabatho, P.K., Parida, B.P., Maphanyane, J.G., 2021. Analysis of the future land use land cover changes in the gaborone dam catchment using CA-markov model: implications on water resources. Rem. Sens. 13, 2427. https://doi.org/10.3390/rs13132427.
Mazor, T., et al., 2021. Future-proofing conservation priorities for sea level rise in coastal urban ecosystems. Biol. Conserv. 260, 260 https://doi.org/10.1016/j.biocon.2021.109190.
Mazor, T., Runting, R.K., Saunders, M.I., Huang, D., Friess, D.A., Nguyen, N.T.H., Lowe, R.J., Gilmour, J.P., Todd, P.A., Lovelock, C.E., 2021. Future-proofing conservation priorities for sea level rise in coastal urban ecosystems. Biol. Conserv. 260, 109190 https://doi.org/10.1016/j.biocon.2021.109190.
Mcleod, E., Poulter, B., Hinkel, J., Reyes, E., Salm, R., 2010. Sea-level rise impact models and environmental conservation: a review of models and their applications. Ocean Coast Manag. 53, 507–517. https://doi.org/10.1016/j.ocecoaman.2010.06.009.
Mendy, P.K., Lobban Jr., Richard, A., 2013. Historical Dictionary of the Republic of Guinea-Bissau (Historical Dictionaries of Africa): Mendy, Peter Karibe, Lobban Jr., Richard A.: 9780810853102: Amazon.Com. Books. Scarecrow Press - ISBN 9780810880276. https://www.amazon.com/Historical-Dictionary-Republic-Guinea-Bissau-Dictionaries/dp/0810853108.
Meyer, W.B., Turner, B.L., 1992. Human population growth and global land-use/cover change. In: Annual Review of Ecology and Systematics. http://www.jstor.org/stable/2097281.
Naturalcapitalproject, 2020. Habitat Quality of InVEST Model. Stanford University. https://naturalcapitalproject.stanford.edu/. (Accessed 18 November 2020). Accessed.
Nicu, I.C., 2021. Is digital shoreline analysis system "fit" for gully erosion assessment? Catena. 203, 105307 https://doi.org/10.1016/j.catena.2021.105307.
Niedertscheider, M., Kuemmerle, T., Muller, D., Erb, K.-H., 2014. Exploring the effects of drastic institutional and socio-economic changes on land system dynamics in Germany between 1883 and 2007. Global Environ. Change 28, 98–108. https://doi.org/10.1016/j.gloenvcha.2014.06.006.
Patrick, C., 1981. National liberation in Portuguese Guinea, 1956-1974. Afr. Aff. 80, 75–99. https://uca.edu/politicalscience/dadm-project/sub-saharan-africa-region/portuguese-guinea-1951-1974/.
Pelissier, Rene, 2004. Guinea-bassau Physical and Social Geography. Africa South of the Sahara 2004, vol. 13. Psychology Press, pp. 526–541. https://www.amazon.com/Historical-Dictionary-Republic-Guinea-Bissau-Dictionaries/dp/0810853108.
Pirasteh, S., Zenner, E.K., Mafi-Gholami, D., Jaafari, A., Kamari, A.N., Liu, G., Zhu, Q., Li, J., 2021. Modeling mangrove responses to multi-decadal climate change and anthropogenic impacts using a long-term time series of satellite imagery. Int. J. Appl. Earth Obs. Geoinf. 102, 102390 https://doi.org/10.1016/j.jag.2021.102390.
pt, Hidrografico, 2021. PREVISÃO DA ALTURA DA MARÉ. Hidrografico Marinha Portugal. https://www.hidrografico.pt/m.mare. (Accessed 11 May 2021). Accessed on.
Ramsar, 2015. The Ramsar Sites Information Service. Ramsar. https://rsis.ramsar.org/about. (Accessed 20 April 2022). Accessed on.
Richards, J., 1999. Remote Sensing Digital Image Analysis, Fifth Edition. Springer, Heidelberg New York Dordrecht London, pp. 1–494. https://doi.org/10.1007/978-3-642-30062-2.
Sajjad, M., Chan, J.C.L., Lin, N., 2020. 18 - modeling of coastal vulnerability to sea-level rise and shoreline erosion using modified CVI model. Environ. Sci. Pol. 106, 99–110. https://doi.org/10.1016/j.envsci.2020.01.004.
Seatemperatureinfo, 2021. Surf Forecast for Bissau. Sea Temperature Info. https://seatemperature.info/bissau-waves-forecast.html. (Accessed 20 April 2021). Accessed on.
Shamsi, S.R.F., 2010. Integrating linear programming and analytical hierarchical processing in raster-GIS to optimize land use pattern at watershed level. J. Appl. Sci. Environ. Manag. 14, 81–85. https://doi.org/10.4314/jasem.v14i2.57868.
Singh, S.K., Mustak, S., Srivastava, P.K., Szabo, S., Islam, T., 2015. Predicting spatial and decadal LULC changes through cellular automata Markov chain models using earth observation datasets and geo-information. Environmental Processes 2, 61–78. https://doi.org/10.1007/s40710-015-0062-x.
Sleeter, B.M., Sohl, T.L., Loveland, T.R., Auch, R.F., Acevedo, W., Drummond, M.A., Sayler, K.L., Stehman, S.V., 2013. Land-cover change in the conterminous United States from 1973 to 2000. Global Environ. Change 23, 733–748. https://doi.org/10.1016/j.gloenvcha.2013.03.006.
Subedi, P., Subedi, K., Thapa, B., 2013. Application of a hybrid cellular automaton – Markov (CA-Markov) model in land-use change prediction: a case study of saddle creek drainage basin, Florida. Appl. Ecol. Environ. Sci. 1, 126–132. https://doi.org/10.12691/aees-1-6-5.

Szlafsztein, C., Sterr, H., 2007. A GIS-based vulnerability assessment of coastal natural hazards, state of Pará, Brazil. J. Coast. Conserv. 11, 53–66. https://doi.org/10.1007/s11852-007-0003-6.

USGS, 2020. Remote Sensing Imagery. Usgs. https://earthexplorer.usgs.gov/. (Accessed 25 May 2020). Accessed on.

Wang, S.W., Gebru, B.M., Lamchin, M., Kayastha, R.B., Lee, W.K., 2020. Land use and land cover change detection and prediction in the kathmandu district of Nepal using remote sensing and GIS. Sustainability 12, 3925. https://doi.org/10.3390/su12093925.

Wu, Z., Han, Z., 2019. Spatial and temporal changes of habitat quality in jiangsu yancheng wetland nayional nature reserve – rare birds of China. Appl. Ecol. Environ. Res. 15, 4807–4821. https://doi.org/10.15666/aeer/1702_48074821.

Xu, L., Liu, X., Tong, D., Liu, Z., Yin, L., Zheng, W., 2022. Forecasting urban land use change based on cellular automata and the PLUS model. Land 11, 652. https://doi.org/10.3390/land11050652.

Yang, Xin, Zheng, Xin-Qi, Lv, L.-N., 2012. A spatiotemporal model of land use change based on ant colony optimization, Markov chain and cellular automata. Ecol. Model. 233, 11–19. https://doi.org/10.1016/j.ecolmodel.2012.03.011.

Yang, S., Zhao, W., Shuai, Y.L., Jing, W., Zhai, W.R., 2018. Influence of land use change on the ecosystem service trade-offs in the ecological restoration area: dynamics and scenarios in the Yanhe watershed, China. Sci. Total Environ. 644, 556–566. https://doi.org/10.1016/j.scitotenv.2018.06.348.

Yirsaw, E., Wu, W., Shi, X., Temesgen, H., Bekele, B., 2017. Land use/land cover change modeling and the prediction of subsequent changes in ecosystem service values in a coastal area of China, the su-Xi-chang region. Sustainability 9, 1–17. https://doi.org/10.3390/su9071204.

Yohannes, H., Soromessa, T., Argaw, M., Dewan, A., 2021. Impact of landscape pattern changes on hydrological ecosystem services in the Beressa watershed of the Blue Nile Basin in Ethiopia. Sci. Total Environ. 793, 148559 https://doi.org/10.1016/j.scitotenv.2021.148559.

Zagórski, P., Jarosz, K., Superson, J., 2020. Integrated assessment of shoreline change along the calypsostranda (svalbard) from remote sensing, field survey and GIS. Mar. Geodes. 43, 433–471. https://doi.org/10.1080/01490419.2020.1715516.

Zhao, L., Peng, Z.-R., 2012. LandSys: an agent-based cellular automata model of land use change developed for transportation analysis. J. Transport Geogr. 25, 35–49. https://doi.org/10.1016/j.jtrangeo.2012.07.006.